

HIGH TEMPERATURE SOLID MECHANICS: MESOSCALE COMPUTATIONAL FORMULATION

Siniša Đ. Mesarović

ABSTRACT. A mesoscale phase field formulation for high temperature computational mechanics of polycrystalline solids with voids is developed. The mathematical description includes translation and rotation of crystalline grains, diffusion through the crystals and interfaces, lattice growth at the boundary and grain boundary sliding, elastic stresses and compositional eigenstrains. The formulation connects heterologous continua; solids are represented by the lattice continuum, while the voids/gas are the standard mass continuum viscous (and elastically compressible) fluid. The deformation gradient for solids is consequently a state variable with evolution defined in the Eulerian sense. We consider non-inertial, controlled-temperature processes with vacancy-atom exchange diffusion mechanism and isotropic interface energies. Nevertheless, as discussed in the concluding section, the formulation provides the basis for extensions to the processes with significant heat sources or sinks, diffusion of multiple species and anisotropic interface energies.

1. Introduction

At high homologous temperatures, the deformation of polycrystalline solids is characterized by diffusion within the crystals, as well as lattice growth/disappearance at the boundary and grain boundary sliding. This is further complicated by: formation of new phases (either controlled by differential diffusion of components or by phase transformation), diffusion-controlled dislocation climb, and nucleation and evolution of voids. A typical example in materials service is creep of metals, alloys and ceramics [2], including creep fracture [6]. In the manufacturing stage, there are sintering and stress-assisted sintering [16], which are an important stage of some additive manufacturing methods [26] and are often accompanied by grain growth and recrystallization [14]. To address these phenomena on the mesoscale, i.e., within crystalline grains and on the grain boundaries, a specialized continuum formulation is needed. A general mathematical formulation for such a mesoscale

2020 *Mathematics Subject Classification:* 74-10, 74A05, 74N25; 74A60, 74C20, 74F05.

Key words and phrases: sintering under stress, creep, grain growth, phase field, lattice continuum.

solid continuum (lattice continuum) has been developed, assuming sharp interfaces between grains, phases and voids [21–23] and used within computational limitations of the sharp interface formulation [18]. However, the problem is characterized by complex 3D geometry and moving boundaries, which makes analytic solutions inaccessible (except for a few special cases) and very difficult to tackle computationally with the sharp interface formulation which requires tracking of curved subspaces of different dimensions [15]. The main goal of this communication is to develop the phase field (diffuse interface) mathematical formulation capable of computational handling of such complex problems. An additional caveat here is that most problems in high temperature solid mechanics require description of voids, i.e., the gas phase. However, the solid and gas phases are described by heterologous¹ continua (lattice and mass continuum).

The paper is organized as follows. In the remainder of this section, we summarize the key points of the lattice continuum formulation as it applies to the bulk of a crystalline solid. In Section 2, we develop the kinematics of the phase field formulation for heterologous continua (lattice and mass) with the focus on lattice growth and grain boundary sliding in the diffuse interface framework. In Section 3, we consider the free energy of the problem and its time derivative, thus revealing the nature of the relevant generalized forces. In Section 4, we analyze the power balance and dissipation for temperature-controlled problems, followed by derivation of governing equations by means of the Principle of virtual power in Section 5. In Section 6, we discuss the expressions for energy densities and provide closure (i.e., the non-dissipative constitutive laws). Section 7 contains an example of dimensional analysis for a specific class of problems. Finally, in Section 8, we discuss the extensions of the present formulation to the processes with significant heat sources or sinks, diffusion of multiple species and anisotropic interface energies.

1.1. Lattice continuum. Standard continuum mechanics formulation (e.g., [19]) is inspired by the flow of fluids. The starting point is the motion of the *material* element where the material is identified with *mass*. In Eulerian (spatial) frame, the material element ρdV , where ρ is the mass density and $dV = dx_1 dx_2 dx_3$, currently at position $\mathbf{x} = (x_1, x_2, x_3)$, moves with the velocity $\mathbf{v}_m(\mathbf{x})$. The entire continuum kinematics and dynamics then follow from this initial definition. In crystalline solids, when diffusion is operational, the mass velocity is different from the lattice velocity [4]; the mass moves with the lattice, and through the lattice. Since most of the traditional (diffusionless) solid mechanics is based on the deformation/motion of the crystal lattice (e.g., elasticity is based on lattice stretching, while dislocation/crystal plasticity is based on the relative translation of lattice parts), it makes little sense to describe solid kinematics using the mass velocity as the primary field. Instead, we identify the *material* with the *lattice*. Then, with lattice density $N(\mathbf{x})$ (the number of lattice sites per unit volume), the material element NdV , currently at position \mathbf{x} , moves with the $\mathbf{v}(\mathbf{x})$. The lattice density and mass density are easily connected if the concentration of different components

¹Heterologous = from different origin.

is known. The mass velocity will depend on the lattice velocity and on the fluxes of different components.

In solids without diffusion, the mass and lattice continua are indistinguishable. The traditional elasticity and crystal plasticity are in fact lattice continua, where distinction between mass and lattice is ignored. When diffusion is present, such distinction is needed. Solid mechanics traditionally relies on Lagrangean (material) frame, with the material point having the reference position \mathbf{X} , the current position $\mathbf{x}(\mathbf{X}, t)$ and the fundamental tensor field being the deformation gradient, with components $F_{ij}(X, t) = \partial x_i / \partial X_j$. The reference position is typically taken to be the initial position or the position at some reference time – in any case, it corresponds to a specific real configuration. However, when lattice grows and disappears at the boundary, the reference configuration for the newly created lattice cannot be determined by physical reasoning. This is illustrated in Figure 1, where new lattice points denoted A are created at some time different from the initial time and have no meaningful reference position, and thus, the deformation gradient is not defined.

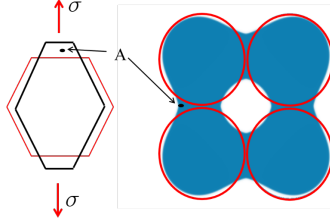


FIGURE 1. Grain in a polycrystal subject to diffusional creep (left), and four particles (grains) sintering (right). The initial shapes are shown in red. The current lattice points A did not exist in the initial geometry. They currently exist as a result of diffusion and lattice growth at boundaries.

Nevertheless, the deformation gradient is needed for the description of lattice elasticity, eigenstrains and plasticity. Therefore, we adopt the Eulerian frame with velocity as the primary variable, as the function of current configuration, $\mathbf{v}(\mathbf{x}, t)$. The deformation gradient now treated as a state variable, moving with the lattice, and function of current coordinates $\mathbf{F}(\mathbf{x}, t)$. It is determined by integrating the velocity gradient $\mathbf{L}(\mathbf{x}, t)$ in time, using the standard continuum relation:

$$(1.1) \quad \dot{\mathbf{F}}(\mathbf{x}, t) = \mathbf{L} \cdot \mathbf{F}, \quad \mathbf{L} = \mathbf{v} \nabla.$$

The dot ($\dot{}$) represents the material derivative, i.e., the time derivative following the material (lattice) point. The dyadic product is written without symbol and the gradient operator (in the current configuration) acts on the available tensor (left or right): $(\mathbf{v} \nabla)_{ij} = \partial v_i / \partial x_j$, $(\nabla \mathbf{v})_{ij} = \partial v_j / \partial x_i$.

The velocity gradient is, as usual, decomposed into the symmetric stretch rate tensor and the antisymmetric spin tensor:

$$\mathbf{L}(\mathbf{x}, t) = \mathbf{D} + \mathbf{W}, \quad \mathbf{D} = \frac{1}{2}(\mathbf{L} + \mathbf{L}^T).$$

In the incipient lattice at the boundary, we assume the continuity of state variables, including the deformation gradient, which determines its value in a newly created lattice at the moment of its creation, given that the value in the adjacent existing lattice is known. Thus, (1.1) provides an implicit mathematical definition of the key Lagrangean concepts: the reference configuration and the deformation gradient tensor field.

To keep the accounting simple, we will only consider plastic deformation at the interfaces, arising from the boundary lattice growth and boundary sliding². Elastic and compositional deformations are present everywhere, representing lattice deformation caused by elastic stresses and by changes in composition due to diffusion.

The deformation gradient is multiplicatively decomposed into plastic, \mathbf{F}^p , and elastic-compositional, \mathbf{F}^* , (pseudo)gradients: $\mathbf{F} = \mathbf{F}^* \cdot \mathbf{F}^p$. While the (pseudo)gradients are incompatible, i.e., they are not gradients of a single-valued vector field, they are subject to the multiplicative decomposition (left and right) into rotation and stretch tensors:

$$\mathbf{F}^* = \mathbf{V}^* \cdot \mathbf{R}^* = \mathbf{R}^* \cdot \mathbf{U}^*, \quad \mathbf{F}^p = \mathbf{V}^p \cdot \mathbf{R}^p = \mathbf{R}^p \cdot \mathbf{U}^p.$$

In the context of lattice continuum, the (pseudo)gradients are interpreted as follows. The inverse of elastic-compositional gradient maps the current configuration ($d\mathbf{x}$) to the intermediate configuration ($d\bar{\mathbf{X}}$):

$$d\bar{\mathbf{X}}(\mathbf{x}) = \mathbf{F}^{*-1}(\mathbf{x}) \cdot d\mathbf{x}.$$

The mapping $\mathbf{F}^{*-1}: \mathbf{x} \rightarrow \bar{\mathbf{X}}$ is not necessarily single-valued. The intermediate configuration $\bar{\mathbf{X}}$ is stress-free and free of compositional strains. The inverse of plastic gradient maps the intermediate configuration onto the reference configuration:

$$d\mathbf{X}(\mathbf{x}) = \mathbf{F}^{p-1}(\bar{\mathbf{X}}(\mathbf{x})) \cdot d\bar{\mathbf{X}}(\mathbf{x}).$$

The total mapping $\mathbf{F}^{-1}: \mathbf{x} \rightarrow \mathbf{X}$ is also not necessarily single-valued.

The rotation tensor \mathbf{R}^* represents lattice rotation, while the product $\mathbf{R}^* \cdot \mathbf{R}^p$ represents mass rotation. The plastic deformation \mathbf{F}^p maps the reference configuration into *isoclinic* intermediate configuration [20]; the lattice does not rotate, it only shifts – one part with respect to the other, but mass (e.g., a line of specific atoms) does rotate. The change of volume between the intermediate and current configurations is given

$$F^* = \det \mathbf{F}^* = \frac{dV}{d\bar{V}} = \frac{\bar{N}}{N}.$$

The velocity gradient is subject to an additive decomposition:

$$\mathbf{L} = \mathbf{v}\nabla = \mathbf{L}^* + \mathbf{L}^p.$$

It is then easily shown that

$$\mathbf{L}^* = \dot{\mathbf{F}}^* \cdot \mathbf{F}^{*-1}, \quad \mathbf{L}^p = \mathbf{F}^* \cdot \dot{\mathbf{F}}^p \cdot \mathbf{F}^{p-1} \cdot \mathbf{F}^{*-1}.$$

²The plastic deformation inside the grains is the result of dislocation motion, both glide and climb. This bulk component of plasticity is identical in sharp interface and phase field formulation and has been studied often [1, 3, 13, 22, 23].

The history of grain boundaries and surfaces encoded in \mathbf{F}^p is not needed during the computation. Thus, the relevant state variable tensor field is the elastic-compositional gradient, which evolves as

$$(1.2) \quad \dot{\mathbf{F}}^* = \mathbf{L}^* \cdot \mathbf{F}^* = (\mathbf{v}\nabla - \mathbf{L}^p) \cdot \mathbf{F}^*.$$

This will be one of the governing equations of the system describing the evolution of the elastic-compositional deformation gradient. The plastic deformation gradient \mathbf{L}^p remains to be defined in the next section.

2. Kinematics of the phase fields and diffusion

In the following phase field formulation, we aim to describe:

- Lattice growth/loss at the grain boundary and grain boundary sliding;
- Solid grain phases and gas (void) phases, whereby solid grains are subject to rigid body translation and rotation, elastic and compositional strains, while the gas phase flows viscously through open pores and is elastically compressible in the closed pores; and,
- Diffusion: in the bulk, along grain interfaces and surfaces, sublimation and condensation.

Let the grain $i = 1, 2, \dots, n_g$ be characterized by the phase field $\phi_i(\mathbf{x})$ and the lattice velocity field $\mathbf{v}_i(\mathbf{x})$. Similarly, the gas phase is characterized by the phase field $\Psi(\mathbf{x})$ and the mass velocity field $\mathbf{v}_G(\mathbf{x})$. Most of the domain consists of regions where one of the phase fields has value 1, while all the other phase fields vanish; the exception lies in the thin boundary layers where one phase transitions into the other. At each point of the continuum, the phase fields satisfy the exclusion condition:

$$(2.1) \quad \sum_{i=1}^{n_g} \phi_i = \Phi, \quad \Phi + \Psi = 1.$$

The overall continuum velocity field is:

$$\mathbf{v}(\mathbf{x}) = \sum_{i=1}^{n_g} \phi_i \mathbf{v}_i + \Psi \mathbf{v}_G.$$

Here we combine heterologous continuum fields (lattice and mass) into a single velocity field, and interpret the physical meaning of the velocity field at each point on the bases of phase fields (e.g., if $\Phi(\mathbf{x}) = 1$ and $\Psi(\mathbf{x}) = 0$, the velocity $\mathbf{v}(\mathbf{x})$ is the lattice velocity).

2.1. Solids and interfaces. We first consider diffusion kinematics in solids. Let c be the number of vacancies per lattice site. Then, the number of atoms per lattice site is $\eta = 1 - c$. Further, let g be the lattice creation rate at the boundary layer defined as the number of lattice sites created per existing lattice site in unit time, so that ηg is the strength of the sink for η . Then, it is shown in [Appendix A](#) that

$$(2.2) \quad \dot{\eta} = \frac{\partial \eta}{\partial t} + \mathbf{v} \cdot \nabla \eta = -F^* \nabla \cdot \mathbf{q} - \eta g,$$

where $\mathbf{q}(\mathbf{x}, t)$ is the atomic flux relative to the lattice motion, given per lattice site.

The lattice creation rate g is intrinsically tied with the evolution of grain phase fields. The boundary velocity (relative to the lattice velocity) at the interface layer between the grain i and the gas is $\dot{\phi}_i/|\nabla\phi_i|$, positive outward from the grain. At the interface between grains i and j , the sum of boundary velocities must match the total local source of lattice sites: $\dot{\phi}_i/|\nabla\phi_i| + \dot{\phi}_j/|\nabla\phi_j| = N^{-1/3}g$, where $N^{-1/3}$ is the lattice parameter. Therefore, at each point of the continuum the following condition must be met:

$$(2.3) \quad \sum_i \frac{\dot{\phi}_i}{|\nabla\phi_i|} = N^{-1/3}g.$$

It is clear from (2.3) that g is not an independent variable and in what follows we will use it only as a placeholder. One should take care not to associate any energy or dissipation with g , to avoid double counting of energy associated with ϕ_i or dissipation associated with $\dot{\phi}_i$. It is interesting to contrast this variable with another dependent variable Ψ in condition (2.1), which will be kept formally as independent, with condition (2.1) enforced by a Lagrange multiplier. The energy associated with the gradient of phase field Ψ will signify the distinction between interface energy between two grains and surface energy of a grain (interface between a grain and the gas). The dissipation associated with $\dot{\Psi}$ will signify the difference in dissipation which accompanies lattice growth on the grain boundary and on the grain surface.

At the boundary between the grains i and j , the unit outer normal to grain i , and the tangential projection tensor are given as

$$\mathbf{n}_{ij} = \frac{\nabla\phi_j - \nabla\phi_i}{|\nabla\phi_j - \nabla\phi_i|} = -\mathbf{n}_{ji}, \quad \mathbf{P}_{ij} = \mathbf{P}_{ji} = \mathbf{I} - \mathbf{n}_{ij}\mathbf{n}_{ij}.$$

To simplify later summations, we set $\mathbf{P}_{ii} = 0$. We define the boundary slip rate $\mathbf{s}_{ij} = -\mathbf{s}_{ji}$, such that

$$\mathbf{s}_{ij} \cdot \mathbf{n}_{ij} = 0, \quad \mathbf{P}_{ij} \cdot \mathbf{s}_{ij} = \mathbf{s}_{ij}.$$

The plastic velocity gradient arises from the lattice growth and grain boundary sliding:

$$(2.4) \quad \mathbf{L}^p|_{\Phi \neq 0} = \sum_i g\mathbf{n}_{iG}\mathbf{n}_{iG} + \frac{1}{2} \sum_i \left[\sum_j (g\mathbf{n}_{ij}\mathbf{n}_{ij} + \mathbf{s}_{ij}\mathbf{n}_{ij}) \right],$$

where \mathbf{n}_{iG} is the unit outer normal to the grain i at the interface with the gas. The description of grain boundary slip and lattice growth is clearly inspired by the descriptions of dislocation glide crystal plasticity [1, 3, 13] and dislocation climb crystal plasticity [22, 23]. However, in contrast to the crystal plasticity, here we choose to describe grain boundary slip and lattice growth on the current configuration, rather than the intermediate one. While differences are not quantitatively significant, the choice still needs to be made. The geometry of grain boundaries is described by 5 parameters and its thermodynamics and kinetics are, at present, far less understood than the thermodynamics and kinetics of slip planes in crystals.

Therefore, referring the quantities g and \mathbf{s}_{ij} to the intermediate configuration would not improve accuracy and would be, at present, an unnecessary complication.

2.2. Gas. In gas, the “plastic” velocity gradient arises from the deviatoric shear flow:

$$\mathbf{L}^p|_{\Psi \neq 0} = \mathbf{L} - \frac{1}{3} \text{tr}(\mathbf{L})\mathbf{I} = \mathbf{v}\nabla - \frac{1}{3}(\nabla \cdot \mathbf{v})\mathbf{I}, \quad \mathbf{L}^*|_{\Psi \neq 0} = \frac{1}{3} \text{tr}(\mathbf{L})\mathbf{I} = \frac{1}{3}(\nabla \cdot \mathbf{v})\mathbf{I}.$$

We can now formulate the general phase field expression for the entire domain:

$$\mathbf{L}^p = \Phi \left(\sum_i g \mathbf{n}_{iG} \mathbf{n}_{iG} + \frac{1}{2} \sum_i \sum_j (g \mathbf{n}_{ij} \mathbf{n}_{ij} + \mathbf{s}_{ij} \mathbf{n}_{ij}) \right) + \Psi \left(\mathbf{v}\nabla - \frac{1}{3}(\nabla \cdot \mathbf{v})\mathbf{I} \right).$$

Then, we can complete (1.2) to formulate the first governing equation of the system describing the evolution of the state variable – the elastic-compositional deformation gradient field:

$$(2.5) \quad \dot{\mathbf{F}}^* = \left[\Phi \left(\mathbf{v}\nabla - \sum_i g \mathbf{n}_{iG} \mathbf{n}_{iG} - \frac{1}{2} \sum_i \sum_j (g \mathbf{n}_{ij} \mathbf{n}_{ij} + \mathbf{s}_{ij} \mathbf{n}_{ij}) \right) + \frac{1}{3} \Psi (\nabla \cdot \mathbf{v}) \mathbf{I} \right] \cdot \mathbf{F}^*.$$

3. Free energy of the system

We consider the Eulerian (spatial) domain V , bounded by the surface ∂V . We expect a variety of boundary conditions: periodic, minimal [24], gas and inert solid. Only the last one requires special treatment as the interface energies between the inert solid boundary and active solid or gas may play a role. We will consider non-inertial viscous flow of compressible gas. Chemical and elastic free energy densities $f(\eta, \phi_i, \Psi)$ and $\mathcal{E}(\mathbf{F}^*, \eta, \phi_i, \Psi)$, are given per unit intermediate volume \bar{V} . The total free energy of the system is

$$(3.1) \quad \mathcal{F} = \int_{\bar{V}} (f + \mathcal{E}) d\bar{V} + \int_V \left[\frac{1}{2} \kappa (\nabla \Psi)^2 + \sum_i \frac{1}{2} \zeta (\nabla \phi_i)^2 \right] dV + \int_{\partial V} \gamma(\Psi) d\partial V.$$

The last integral exists only on the inert solid boundary. The material derivative of the free energy can be written as (Appendix B):

$$(3.2) \quad \dot{\mathcal{F}} = \int_V \left[-M^0 \nabla \cdot \mathbf{q} + \mathcal{M}^0 \dot{\Psi} + \tilde{\boldsymbol{\sigma}} : (\mathbf{v}\nabla) - \frac{1}{2} \sum_i \sum_j \mathbf{t}_{ij}^t \cdot \mathbf{s}_{ij} + \sum_i \mu_i^0 \dot{\phi}_i \right] dV \\ + \int_{\partial V} \left[\Upsilon^0 \dot{\Psi} + \sum_i \chi_i^0 \dot{\phi}_i \right] d\partial V.$$

Here, the augmented stress $\tilde{\boldsymbol{\sigma}}$ includes the standard Cauchy stress $\boldsymbol{\sigma}$ and the capillary stresses [7]

$$(3.3) \quad \boldsymbol{\sigma} = \frac{1}{F^*} \frac{\partial \mathcal{E}}{\partial \mathbf{F}^*} \cdot \mathbf{F}^{*T}, \quad \tilde{\boldsymbol{\sigma}} = \boldsymbol{\sigma} - \kappa \nabla \Psi \nabla \Psi - \sum_i \zeta \nabla \phi_i \nabla \phi_i.$$

The shear traction expanding power on the boundary slip rate are

$$\mathbf{t}_{ij}^t = \mathbf{P}_{ij} \cdot \boldsymbol{\sigma} \cdot \mathbf{n}_{ij},$$

where we note that $\mathbf{t}_{ij}^t \cdot \mathbf{s}_{ij} = \mathbf{t}_{ji}^t \cdot \mathbf{s}_{ji}$. Further, we define diffusion potential and phase field potentials as

$$\begin{aligned}
 M^0 &= \frac{\partial(f + \mathcal{E})}{\partial\eta}, \\
 \mu_i^0 &= \frac{1}{F^*} \frac{\partial(f + \mathcal{E})}{\partial\phi_i} - \frac{1}{F^*} \frac{\partial(f + \mathcal{E})}{\partial\eta} \frac{\eta N^{1/3}}{|\nabla\phi_i|} - \frac{t^n N^{1/3}}{|\nabla\phi_i|} - \zeta \nabla^2 \phi_i, \\
 \mathcal{M}^0 &= \frac{1}{F^*} \frac{\partial(f + \mathcal{E})}{\partial\Psi} - \kappa \nabla^2 \Psi.
 \end{aligned}
 \tag{3.4}$$

To understand the physical meaning of the solid phase potential μ_i^0 , it is instructive to compare (qualitatively!) the terms in the phase field expression (other than the Laplacian term which arises as the result of diffuse nature of the interface) to the sharp interface formulation of lattice continuum [21]. The potential μ_i^0 is the power conjugate to $\dot{\phi}_i$ and therefore represents the energetic changes associated with the creation of a new lattice. The term with the normal traction t^n (defined in Appendix B) gives the power expanded by normal tractions. The first term is the energy required for the creation of the new lattice and the 2nd term is the energy change of the existing lattice when the atoms needed for the new lattice are taken out of it. The boundary terms in (3.2), with

$$\Upsilon^0 = \kappa \mathbf{n} \cdot \nabla \Psi + \frac{\partial\gamma}{\partial\Psi}, \quad \chi_i^0 = \zeta \mathbf{n} \cdot \nabla \phi_i,$$

exist only on the inert solid boundary. Their physical meaning is explained in the context of capillary flow on inert solid surfaces [8].

4. Power balance and dissipation

We consider a temperature-controlled process, where temperature is a prescribed field (not necessarily constant, nor uniform). The amount of heat added to the system to bring it into the creep or sintering temperature ranges is much larger than any heat generated in dissipative processes. Formally, the treatment is the same as that for an isothermal process. The second law of thermodynamics then requires non-negative dissipation, $\mathcal{D} \geq 0$, and the power balance is expressed as:

$$\int_{\partial V} \mathbf{t} \cdot \mathbf{v} d\partial V = \dot{\mathcal{F}} + \mathcal{D},
 \tag{4.1}$$

where \mathbf{t} is the boundary traction vector.

Dissipation arises from diffusion, phase propagation (lattice growth), grain boundary sliding and viscous flow of the gas. To describe the viscous flow, we define the viscous stretch rate tensor

$$\mathbf{D} = \frac{1}{2}(\mathbf{L}^p + \mathbf{L}^{pT}).$$

The total dissipation rate is written as

$$\mathcal{D} = \int_V \left[\mathbf{Q} \cdot \mathbf{q} + \mathcal{M} \dot{\Psi} + \sum_i \mu_i \dot{\phi}_i + \boldsymbol{\tau} : \mathbf{D} + \sum_i \sum_j \mathbf{S}_{ij} \cdot \mathbf{s}_{ij} \right] dV
 \tag{4.2}$$

$$+ \int_{\partial V} \sum_i \Upsilon_i \dot{\phi}_i d\partial V \geq 0.$$

The second law will be satisfied for:

$$(4.3) \quad \begin{aligned} \dot{\phi}_i &= b_S \mu_i, \quad \dot{\Psi} = b_G \mathcal{M}, \quad \dot{\phi}_i = \beta \Upsilon_i \text{ on } \partial V, \quad b_S, b_G, \beta > 0 \\ \boldsymbol{\tau} &= 2\omega(\Phi, \Psi) \mathbf{D}, \quad \omega = \Phi \omega_S + \Psi \omega_G > 0, \quad \mathbf{s}_{ij} = s_y \left| \frac{\mathbf{S}_{ij}}{S_y} \right|^{H-1} \frac{\mathbf{S}_{ij}}{S_y}, \quad H \gg 1, \\ \mathbf{q} &= \mathbf{B} \cdot \mathbf{Q} \quad \text{where } \mathbf{B} \text{ is positive definite.} \end{aligned}$$

The mobilities b_s and b_G enable different dissipation for grain boundary growth at grain boundaries and free surfaces, $\boldsymbol{\tau}$ is the viscous stress tensor and the viscosity function $\omega(\Phi, \Psi)$ is defined in such a way that the viscous flow in solids is negligible: $\omega_S \gg \omega_G$. The diffusional mobility tensor \mathbf{B} should enable bulk, interface and surface diffusion, as well as sublimation – diffusion through gas – condensation:

$$(4.4) \quad \begin{aligned} \mathbf{B} &= B_0 \mathbf{I} + \sum_i \left(B_{SS} \sum_j \mathbf{P}_{ij} + B_{SG} \mathbf{P}_{iG} \right), \\ B_0 &= \Phi B_0^S + \Psi B_0^G, \quad \mathbf{P}_G = \mathbf{I} - \mathbf{n}_{iG} \mathbf{n}_{iG}, \end{aligned}$$

where $\mathbf{P}_{ii} = 0$, B_0 is the mobility in the bulk, while B_{SS} and B_{SG} are the mobilities along solid-solid and solid-gas boundaries. To disable sublimation and diffusion through the gas, one sets $B_0^G = 0$. The constitutive law for the grain boundary slip, assumed without reference to any particular atomic scale mechanism [11], is the viscous regularization of the ideal rate-independent yield condition with the yield stress S_y and a large power H . The boundary terms (∂V) in (4.2) and (4.3) are associated with the mobility of the triple line [8] between the solids, gas and the inert solid boundary.

The power balance (4.1) can then be written as

$$\begin{aligned} & \int_{\partial V} \left[\mathbf{t} \cdot \mathbf{v} + \sum_i (\Upsilon^0 - \Upsilon_i - \chi_i^0) \dot{\phi}_i \right] d\partial V \\ &= \int_V \left[(\mathbf{Q} + \nabla M^0) \cdot \mathbf{q} + (\mathcal{M} + \mathcal{M}^0) \dot{\Psi} + \sum_i (\mu_i + \mu_i^0) \dot{\phi}_i \right. \\ & \quad \left. + \boldsymbol{\Sigma} : (\mathbf{v} \nabla) + \frac{1}{2} \sum_i \sum_j (\mathbf{S}_{ij} - \mathbf{t}_{ij}^t) \cdot \mathbf{s}_{ij} \right] \end{aligned}$$

where

$$\boldsymbol{\Sigma} = \tilde{\boldsymbol{\sigma}} + \boldsymbol{\tau}.$$

For all boundary conditions listed at the beginning of Section 3, the conservation of solid matter is enforced, either locally or globally:

$$(4.5) \quad \mathbf{n} \cdot \mathbf{q}|_{\partial V} = 0 \quad \text{or} \quad \int_{\partial V} \mathbf{n} \cdot \mathbf{q} d\partial V = 0.$$

5. Principle of virtual power and governing equations

To formulate the principle of virtual power [9, 10, 23], an additional constraint is needed:

$$(5.1) \quad \int_V \lambda \left(\dot{\Psi} + \sum_i \dot{\phi}_i \right) dV = 0,$$

where λ is the Lagrange multiplier. We then consider independent variations (test functions): $\hat{\mathbf{v}}$, $\hat{\mathbf{q}}$, $\hat{\mathbf{s}}_{ij}$, $\hat{\Psi}$, and $\hat{\phi}_j$ ($i, j = 1, 2, \dots, n_g$), so that the statement of the principle of virtual power is expressed as:

$$\begin{aligned} & \int_{\partial V} \left[(\mathbf{t} - \mathbf{n} \cdot \boldsymbol{\Sigma}) \cdot \hat{\mathbf{v}} - \sum_j (\Upsilon_j - \Upsilon^0 - \chi_j^0) \hat{\phi}_j \right] d\partial V \\ &= \int_V \left[(\mathbf{Q} + \nabla M^0) \cdot \hat{\mathbf{q}} - (\nabla \cdot \boldsymbol{\Sigma}) \cdot \hat{\mathbf{v}} + \frac{1}{2} \sum_i \sum_j (\mathbf{S}_{ij} - \mathbf{t}_{ij}^t) \cdot \hat{\mathbf{s}}_{ij} \right. \\ & \quad \left. + [\mathcal{M} + \mathcal{M}^0 - \lambda] \hat{\Psi} + \sum_j (\mu_j + \mu_j^0 - \lambda) \hat{\phi}_j \right] dV. \end{aligned}$$

Then, for arbitrary test functions, the following conditions must be satisfied in V :

$$(5.2) \quad \mathbf{Q} = -\nabla M^0, \quad \mathcal{M} = -\mathcal{M}^0 + \lambda, \quad \mu_j = -\mu_j^0 + \lambda, \quad \nabla \cdot \boldsymbol{\Sigma} = 0, \quad \mathbf{S}_{ij} = \mathbf{t}_{ij}^t.$$

At the domain boundary ∇V , we may have:

- Natural boundary conditions $\mathbf{t} = \mathbf{n} \cdot \boldsymbol{\Sigma}$, or essential boundary conditions for \mathbf{v} .
- Natural boundary conditions for vanishing $\mathbf{n} \cdot \mathbf{B} \cdot \nabla M^0$ locally or globally (4.5), and/or, the essential boundary conditions $\eta = 0$ in a gas which does not accept solid atoms.
- Natural boundary conditions $\Upsilon_j = \Upsilon^0 + \chi_j^0$ and/or essential boundary conditions for ϕ_j .

From (5.2), the field equations for the phase fields are written as

$$\dot{\phi}_i = b_S(-\mu_i^0 + \lambda), \quad \dot{\Psi} = b_G(-\mathcal{M}^0 + \lambda).$$

Upon eliminating λ by means of (2.1) (Appendix C), we obtain

$$\begin{aligned} \dot{\phi}_i &= -b_S \mu_i^0 + \frac{b_S^2}{b_G + b_S n_g} \sum_j \mu_j^0 + \frac{b_S b_G}{b_G + b_S n_g} \mathcal{M}^0 \\ \dot{\Psi} &= \left(\frac{b_G^2}{b_G + b_S n_g} - 1 \right) \mathcal{M}^0 + \frac{b_G b_S}{b_G + b_S n_g} \sum_j \mu_j^0 \end{aligned}$$

where n_g is the number of solid phase fields. The governing equations for the unknown fields \mathbf{F}^* , η , ϕ_i ($i = 1, \dots, n_g$), Ψ and \mathbf{v} are:

$$\dot{\mathbf{F}}^* = \left[\Phi \left(\mathbf{v} \nabla - \sum_i g \mathbf{n}_{iG} \mathbf{n}_{iG} - \frac{1}{2} \sum_i \sum_j (g \mathbf{n}_{ij} \mathbf{n}_{ij} + \mathbf{s}_{ij} \mathbf{n}_{ij}) \right) + \frac{1}{3} \Psi (\nabla \cdot \mathbf{v}) \mathbf{I} \right] \cdot \mathbf{F}^*,$$

$$\begin{aligned}
\dot{\eta} &= F^* \nabla \cdot \left[\mathbf{B} \cdot \nabla \frac{\partial(f + \mathcal{E})}{\partial \eta} \right] - \eta g, \\
(5.3) \quad \dot{\phi}_i &= -b_S \mu_i^0 + \frac{b_S^2}{b_G + b_S n_g} \sum_j \mu_j^0 + \frac{b_S b_G}{b_G + b_S n_g} \mathcal{M}^0, \quad i = 1, 2, \dots, n_g, \\
\dot{\Psi} &= \left(\frac{b_G^2}{b_G + b_S n_g} - 1 \right) \mathcal{M}^0 + \frac{b_G b_S}{b_G + b_S n_g} \sum_j \mu_j^0, \\
\nabla \cdot \left(\boldsymbol{\sigma} + \boldsymbol{\tau} - \kappa \nabla \Psi \nabla \Psi - \sum_j \zeta \nabla \phi_j \nabla \phi_j \right) &= 0
\end{aligned}$$

where μ_i^0 and \mathcal{M}^0 are given in (3.4) and

$$\begin{aligned}
g &= \frac{\bar{N}^{1/3}}{F^{*1/3}} \sum_i \frac{1}{|\nabla \phi_i|} \left[-b_S \mu_i^0 + \frac{b_S^2}{b_G + b_S n_g} \sum_j \mu_j^0 + \frac{b_S b_G}{b_G + b_S n_g} \mathcal{M}^0 \right], \\
\mathbf{s}_{ij} &= \frac{s_y}{S_y} \left| \frac{\mathbf{t}_{ij}^t}{S_y} \right|^{H-1} \mathbf{t}_{ij}^t, \quad \mathbf{t}_{ij}^t = \mathbf{P}_{ij} \cdot \boldsymbol{\sigma} \cdot \mathbf{n}_{ij}.
\end{aligned}$$

6. Energy densities

The chemical free energy density $f(\eta, \phi_i, \Psi)$ for the entire domain is written as the linear combination of phase contributions, with addition of energy barriers between the phases:

$$\begin{aligned}
f(\eta, \phi_i, \Psi) &= \sum_{i=1}^{n_g} [\phi_i f_i(\eta) + \Delta f_i w(\phi_i)] + \Psi f_G(\eta) + \Delta f_G w(\Psi), \\
w(\phi_i) &= 16 \phi_i^2 (1 - \phi_i)^2.
\end{aligned}$$

The energy barriers, Δf_i and Δf_G , and the phase field parameters, ζ and κ (3.1), are computed from physical quantities – solid-solid and solid gas interface energies Γ_{SS} and Γ_{SG} , and the computational parameter – the nominal interface thickness h (Appendix D):

$$\begin{aligned}
(6.1) \quad \Delta f_i &= \frac{3}{8} \frac{\Gamma_{SS}}{h}, & \Delta f_G &= \frac{3}{4} \frac{\Gamma_{SG}}{h} - \frac{3}{8} \frac{\Gamma_{SS}}{h}, \\
\zeta &= \frac{3}{4} \Gamma_{SS} h, & \kappa &= \frac{3}{2} \Gamma_{SG} h - \frac{3}{4} \Gamma_{SS} h.
\end{aligned}$$

In the case of inert solid boundary condition (b), with interface energies Γ_{Sb} and Γ_{Gb} , the domain boundary interface energy is

$$\gamma(\Psi) = (1 - \Psi) \Gamma_{Sb} + \Psi \Gamma_{Gb}.$$

If only one species of solid atoms is present and diffusion is based on the atom-vacancy exchange mechanisms, the chemical free energy of solids is the energy of mixing, for which the regular solution model [12] can be used. Let the equilibrium vacancy concentration at the given temperature T and pressure p be denoted

$c_{eq}(T, p)$. Then, for small departures from equilibrium concentration, the regular solution model can be approximated [21]:

$$f_i(\eta) = \frac{1}{2} \frac{kT\bar{N}}{c_{eq}(T, p)} (c - c_{eq}(T, p))^2 = \frac{1}{2} \frac{kT\bar{N}}{(1 - \eta_{eq}(T, p))} (\eta - \eta_{eq}(T, p))^2,$$

where k is the Boltzmann constant and $\eta_{eq} = 1 - c_{eq}$. In the absence sublimation of solid atoms and transport through the gas, the chemical energy density of the gas can be ignored: $f_G(\eta) = 0$. Then the partials needed for diffusion and phase potentials (3.4) are:

$$\begin{aligned} \frac{\partial f}{\partial \eta} &= \sum_{i=1}^{n_g} \phi_i f'_i(\eta) = \sum_{i=1}^{n_g} \phi_i \frac{kT\bar{N}}{(1 - \eta_{eq}(T, p))} (\eta - \eta_{eq}(T, p)) + \Psi f'_G(\eta), \\ \frac{\partial f}{\partial \Psi} &= f_G(\eta) + \delta f_G w'(\Psi), \\ \frac{\partial f}{\partial \phi_i} &= \sum_{i=1}^{n_g} [f_i(\eta) + \Delta f_i w'(\phi_i)], \end{aligned}$$

where the prime superposed on the function of a single variable means the derivative with respect to that variable.

Depending on the complexity and the importance of gas compressibility, the elasticcompositional energy density $\mathcal{E}(\mathbf{F}^*, \eta, \phi_i, \Psi)$ can be represented as the weighted sum of solid and gas energies: $\mathcal{E} = \sum_i \phi_i \mathcal{E}_S + \Psi \mathcal{E}_G$. Here, we choose a simpler formulation where the gas compressibility is linear. Accordingly, both the solid and the gas can be described as elastic and viscous, but with parameters depending on the phase, so that elasticity is dominant in solids and volumetric gas deformation, while viscosity is dominant in deviatoric gas deformation. The elastic-compositional energy can then be considered as a function of an appropriate strain measure \mathbf{E} : $\mathcal{E}(\eta, \mathbf{E}, \phi_i, \Psi)$. Here, we choose the Green strain tensor:

$$\mathbf{E} = \frac{1}{2} (\mathbf{F}^{*T} \cdot \mathbf{F}^* - \mathbf{I}).$$

Irrespective of the choice of strain measure, the strain \mathbf{E} is expected to be small and is expressed as the sum of the compositional eigenstrain $\boldsymbol{\varepsilon}$ and the elastic strain, both of which are small. Typically, a change in vacancy concentration produces only stress-free volume change, so that the compositional eigenstrain is assumed to be purely volumetric and proportional to the change in vacancy concentration. We assume linear elasticity, so that the elastic energy is given in the quadratic form:

$$\mathcal{E} = \frac{1}{2} (\mathbf{E} - \boldsymbol{\varepsilon}) : \mathbf{C}(\phi_i, \Psi) : (\mathbf{E} - \boldsymbol{\varepsilon}), \quad \boldsymbol{\varepsilon} = \alpha(\eta - \eta_0) \mathbf{I},$$

where $\eta_0 = 1 - c_0 = \eta_{eq}(T_0, p_0)$ is the equilibrium value of $(1 - c)$ at the reference temperature T_0 and the reference pressure p_0 . The isotropic elasticity tensor can be expressed in terms of the bulk and shear moduli:

$$\begin{aligned} C_{ijkl} &= K \delta_{ij} \delta_{kl} + G \left(\delta_{ik} \delta_{jl} + \delta_{il} \delta_{jk} - \frac{2}{3} \delta_{ij} \delta_{kl} \right), \\ K &= \Phi K_S + \Psi K_G, \quad G = \Phi G_S + \Psi G_G, \\ \mathbf{C} &= \Phi \mathbf{C}_S + \Psi \mathbf{C}_G, \end{aligned}$$

where $G_G \gg G_S$ and $K_G < K_S$. The partial derivatives needed for the potentials (3.4) are therefore:

$$\begin{aligned}\frac{\partial \mathcal{E}}{\partial \eta} &= -\alpha \mathbf{I} : \mathbf{C} : (\mathbf{E} - \boldsymbol{\varepsilon}), \\ \frac{\partial \mathcal{E}}{\partial \phi_i} &= \frac{1}{2} (\mathbf{E} - \boldsymbol{\varepsilon}) : (\mathbf{C}_S - \mathbf{C}_G) : (\mathbf{E} - \boldsymbol{\varepsilon}), \\ \frac{\partial \mathcal{E}}{\partial \Psi} &= \frac{1}{2} (\mathbf{E} - \boldsymbol{\varepsilon}) : (\mathbf{C}_G - \mathbf{C}_S) : (\mathbf{E} - \boldsymbol{\varepsilon}).\end{aligned}$$

To complete the formulation, we need an expression for the Cauchy stress $\boldsymbol{\sigma}$ in (5.3). To that end, we note that the expression $\mathbf{C} : (\mathbf{E} - \boldsymbol{\varepsilon})$ is, in fact, the 2nd Piola–Kirchhoff stress tensor referred to the intermediate configuration (i.e., the work conjugate of the elastic Green strain), so that the Cauchy stress is given as

$$\boldsymbol{\sigma} = \frac{1}{F^*} \frac{\partial \mathcal{E}}{\partial \mathbf{F}^*} \cdot \mathbf{F}^{*T} = \frac{1}{F^*} \mathbf{F}^{*T} \cdot \left[\mathbf{C} : \left(\frac{1}{2} (\mathbf{F}^{*T} \cdot \mathbf{F}^* - \mathbf{I}) - \alpha (\eta - \eta_0) \mathbf{I} \right) \right] \cdot \mathbf{F}^*.$$

7. Elements of dimensional analysis

The nonlinearity and complexity of the governing equations (5.3) indicate computational approach. In such cases, dimensional analysis can provide some useful insights into the parameters used and the competition between the physical processes. Depending on the problem at hand, different characteristic lengths, times and forces can be defined. Here, we focus on the phase field and diffusion equations (second, third and fourth equations in (5.3)), as the analysis of the other two equations is rather simple. Moreover, we focus on a specific problem – early stages of sintering, which will govern our choices of characteristic quantities.

The phase field equations indicate the characteristic length of the process – the nominal interface thickness h . The sintering is driven by the difference between solid-gas and solid-solid interface energies (6.1), so that the characteristic force is $(\Gamma_{SG} - \Gamma_{SS})h$. In the early stages of sintering, the material is mostly transported from one part of the solid-gas interface to the other. This the relevant phase field and diffusion mobilities (4.3), (4.4) are b_G and B_{SG} . The analysis of the phase field equations then yields the characteristic lattice growth time

$$\mathcal{T}_{\text{lg}} = \frac{h}{b_G(\Gamma_{SG} - \Gamma_{SS})}.$$

Denoting the nondimensional quantities with a concave arc (e.g., $\check{t} = t/\mathcal{T}_{\text{lg}}$, $\check{\Delta} = h\nabla$), the nondimensional diffusion and phase field equations can then be written as

$$\begin{aligned}\frac{d\eta}{d\check{t}} &= F^* \frac{\mathcal{T}_{\text{lg}}}{\mathcal{T}_{\text{diff}}} \check{\nabla} \cdot \left[\check{\mathbf{B}} \cdot \check{\nabla} \frac{\partial(\check{f} + \check{\mathcal{E}})}{\partial \eta} \right] - \eta \check{g}, \\ \frac{d\phi_i}{d\check{t}} &= -\check{b}_S \check{\mu}_i^0 + \frac{\check{b}_S^2}{1 + \check{b}_S n_g} \sum_j \check{\mu}_j^0 + \frac{\check{b}_S}{1 + \check{b}_S n_g} \check{\mathcal{M}}^0,\end{aligned}$$

$$\frac{d\Psi}{dt} = \frac{-\check{b}_S}{1 + \check{b}_S n_g} \check{\mathcal{M}}^0 + \frac{\check{b}_S}{1 + \check{b}_S n_g} \sum_j \check{\mu}_j^0.$$

$$\check{g} = \frac{h\bar{N}^{1/3}}{F^{*1/3}} \sum_i \frac{1}{|\check{\nabla}\phi_i|} \frac{d\phi_i}{d\check{t}},$$

where the characteristic diffusion time is given by

$$\mathcal{T}_{\text{diff}} = \frac{1}{hB_{SG}(\Gamma_{SG} - \Gamma_{SS})},$$

and the nondimensional quantity $h\bar{N}^{1/3}$ represents the number of lattice points fitting into the phase field interface width. The ratio $\mathcal{T}_{\text{lg}}/\mathcal{T}_{\text{diff}}$ determines which physical process governs the overall sintering rate. For example, if $\mathcal{T}_{\text{lg}}/\mathcal{T}_{\text{diff}} < 1$, the sintering rate is governed by diffusion and not by the boundary dissipation required for lattice growth. Clearly, the definitions of both characteristic times are predicated by our (informed) choice of dominant diffusion/lattice growth mechanism. For example, Nabarro–Herring creep problem in polycrystals will have \mathcal{T}_{lg} depending on b_S and $\mathcal{T}_{\text{diff}}$ on the bulk mobility in solids B_0^S (4.4). Such a problem has been discussed (albeit in the sharp interface context) in [21].

8. Discussion and extensions

The derived system of governing equations (5.3) represents a system of $n_g + 14$ scalar partial differential equations for as many unknown fields: \mathbf{F}^* , η , ϕ_i ($i = 1, \dots, n_g$), Ψ , and \mathbf{v} . In anticipation of the numerical treatment, e.g., spatial discretization by the finite element method, we have already written the 4th order p.d.e's for ϕ_i ($i = 1, \dots, n_g$) and Ψ as pairs of 2nd order equations, so that the potentials μ_i^0 ($i = 1, \dots, n_g$) and \mathcal{M}^0 are treated as independent variables with corresponding additional equations (3.4). The size of the system is then $2n_g + 15$. The discrete finite element system with n_{Nod} will then consist of $n_{\text{Nod}}(n_g + 11)$ ordinary differential equations (in time) and $n_{\text{Nod}}(n_g + 14)$ algebraic equations (to be enforced at any time), for nodal variables as functions of time.

The nonlinear system (5.3) represents the full range of motion of the grains (rotations and translations) as well as the lattice growth at the boundaries and grain boundary sliding. The system also allows for all possible diffusion paths (crystal bulk, grain boundary, free surface). While most of the closure equations (constitutive laws) are linear – the exception being the grain boundary sliding in (4.3) – the problem is still intractable analytically and requires computational approach.

We have considered a relatively simple system with a single lattice geometry and the lattice occupied either by vacancies or one species of atoms. Interstitial diffusion typically has different thermodynamics and kinetics from the vacancy diffusion considered here. To describe this type of diffusion, the lattice of interstices is added to the base lattice to form a complex lattice, and the bookkeeping for the two lattices is kept separate. Such a method has been employed by [17] to address the problem of ordered compounds – metal carbides, whereby carbon diffuses only along the carbon site lattice, which is the interstitial lattice to the metal lattice.

While the number of unknowns increases with the number of diffusion species, this does not present a conceptual problem, but merely an extra bookkeeping effort.

The formation of new phases, dictated by the disparities in the diffusion rates of different species, is a more complex problem. It requires the definition of eigenstrains associated with martensitic phase transformations. Such strains and rotations are often not small. This problem is partially addressed by [17], who used the spatial averaging of the lamellar phase structure to simplify the problem. Nevertheless, the treatment presented here includes arbitrary deformation and rotation, and is thus amenable to inclusion of eigen-gradient associated with the martensitic transformation (in addition to compositional eigenstrain), e.g.,

$$\mathbf{F}^* = \mathbf{F}^{el} \cdot \mathbf{F}^{\text{eigen}},$$

where $\mathbf{F}^{\text{eigen}}$ now includes both compositional volumetric strain and transformation strain and rotation, and the Green strain is

$$\mathbf{E} = \frac{1}{2}(\mathbf{F}^{elT} \cdot \mathbf{F}^{el} - \mathbf{I}).$$

We have also assumed a controlled-temperature process, treated formally as an isothermal process. This amounts to the assumption that any heat resulting from dissipation is negligible compared to the amount of heat used to heat the solid externally and is quickly transported away without causing only negligible local temperature changes. The temperature is considered an externally imposed global parameter, $T(t)$. While we have suppressed temperature dependence in our notation, all parameters can, in principle, be temperature dependent. For the class of processes considered here, this is justified. However, should the problem include significant heat sources, such as exothermic/endothermic transformations, heat conduction should be included in the formulation (heat convection is already included by simply treating the temperature as a material field).

Finally, the dependence of interface energies on the misorientation of grains and the orientation of the interface planes, is very important for the grain growth process which often accompanies high temperature processes in polycrystalline solids. Attempts have been made in the literature to simulate grain growth with anisotropic interface energies [5, 25, 27], but none of them include the description of grain translation and rotation, i.e., each crystal is assumed to have a fixed orientation in space and each initial material point has a fixed position. This is a challenging problem as the interface geometry is a function of 5 scalar parameters. Tracking such a parameter dependence in time requires tracking the grain rotations and interface rotations.

Acknowledgments. This work was supported by: US Army Research Laboratory Cooperative Agreement W911NF-23-2-0087, US National Center of Manufacturing Sciences Collaborative Agreement 2024053-143006 and US National Science Foundation Award 2328678.

Appendix A. Diffusion

The lattice site density evolves as

$$(A.1) \quad \frac{\partial N}{\partial t} = -\nabla \cdot (N\mathbf{v}) + N_g$$

But the number of atoms depends on the atomic velocity \mathbf{v}^a :

$$\frac{\partial}{\partial t}(N\eta) = \frac{\partial N}{\partial t}\eta + N\frac{\partial \eta}{\partial t} = -\nabla \cdot (\eta N\mathbf{v}^a),$$

whence, upon substituting (A.1)

$$\begin{aligned} & -\eta\nabla \cdot (N\mathbf{v}) + \eta N g + N\frac{\partial \eta}{\partial t} = \nabla \cdot (\eta N\mathbf{v}^a) \\ \Rightarrow & N\mathbf{v} \cdot \nabla \eta + \eta N g + N\frac{\partial \eta}{\partial t} = -\nabla \cdot (\eta N(\mathbf{v}^a - \mathbf{v})) \\ \Rightarrow & \dot{\eta} = \frac{\partial \eta}{\partial t} + \mathbf{v} \cdot \nabla \eta = -\frac{1}{N}\nabla \cdot (\eta N(\mathbf{v}^a - \mathbf{v})) - \eta g. \end{aligned}$$

Finally, we note that $N = \bar{N}/F^*$, where \bar{N} is constant, and define the flux as

$$\mathbf{q} = \frac{\eta}{F^*}(\mathbf{v}^a - \mathbf{v}),$$

to obtain

$$\dot{\eta} = -F^*\nabla \cdot \mathbf{q} - \eta g.$$

Appendix B. Free energy rate

Starting from (3.1):

$$\mathcal{F} = \int_V (f + \mathcal{E})dV + \int_V \left[\frac{1}{2}\kappa(\nabla\Psi)^2 + \sum_i \frac{1}{2}\zeta(\nabla\phi_i)^2 \right]dV + \int_{\partial V} \gamma(\Psi)d\partial V,$$

the time derivative in the fixed Eulerian volume is

$$\begin{aligned} \dot{\mathcal{F}} = & \int_V \frac{1}{F^*} \left[\frac{\partial(f + \mathcal{E})}{\partial \eta} \dot{\eta} + \frac{\partial(f + \mathcal{E})}{\partial \Psi} \dot{\Psi} + \frac{\partial \mathcal{E}}{\partial \mathbf{F}^*} : \dot{\mathbf{F}}^{*T} + \sum_i \frac{\partial(f + \mathcal{E})}{\partial \phi_i} \dot{\phi}_i \right] dv \\ & + \int_V \left[\kappa \nabla \Psi \cdot \overline{\dot{\nabla \Psi}} + \sum_i \zeta \nabla \phi_i \cdot \overline{\dot{\nabla \phi_i}} \right] dV + \int_{\partial V} \frac{\partial \gamma}{\partial \Psi} \dot{\Psi} d\partial V. \end{aligned}$$

Next, the material derivative of a gradient can be written as

$$\overline{\dot{\nabla \phi}} = \nabla \dot{\phi} - (\nabla \phi) \cdot (\mathbf{v} \nabla),$$

so that:

$$\begin{aligned} \nabla \phi_i \cdot \overline{\dot{\nabla \phi_i}} &= \nabla \phi_i \cdot \nabla \dot{\phi}_i - (\nabla \phi_i \nabla \phi_i) : (\mathbf{v} \nabla) \\ &= \nabla \cdot (\dot{\phi}_i \nabla \phi_i) - \dot{\phi}_i \nabla^2 \phi_i - (\nabla \phi_i \nabla \phi_i) : (\mathbf{v} \nabla). \end{aligned}$$

Then, using (1.2), (2.2), (2.3) and (2.4) and defining the Cauchy stress as in (3.3), we obtain

$$\dot{\mathcal{F}} = \int_V \left[-\frac{\partial(f + \mathcal{E})}{\partial \eta} \frac{1}{F^*} F^* \nabla \cdot \mathbf{q} + \left[\frac{1}{F^*} \frac{\partial(f + \mathcal{E})}{\partial \Psi} - \kappa \nabla^2 \Psi \right] \dot{\Psi} \right. \\ \left. + \sum_i \left[\frac{\partial(f + \mathcal{E})}{\partial \phi_i} \nabla \cdot \dot{\phi}_i - \dot{\phi}_i \nabla^2 \phi_i - (\nabla \phi_i \nabla \phi_i) : (\mathbf{v} \nabla) \right] \right] dv$$

$$\begin{aligned}
& + \left[\boldsymbol{\sigma} - \kappa(\nabla\Psi\nabla\Psi) - \sum_i \zeta(\nabla\phi_i\nabla\phi_i) \right] : (\mathbf{v}\nabla) - \frac{1}{2} \sum_i \sum_j \boldsymbol{\sigma} : \mathbf{n}_{ij} \mathbf{s}_{ij} \\
& + \sum_i \left[\frac{1}{F^*} \frac{\partial(f+\mathcal{E})}{\partial\phi_i} - \frac{1}{F^*} \frac{\partial(f+\mathcal{E})}{\partial\eta} \frac{\eta N^{1/3}}{|\nabla\phi_i|} \right. \\
& - \left. \left(\sum_j \boldsymbol{\sigma} : \mathbf{n}_{jG} \mathbf{n}_{jG} + \frac{1}{2} \sum_j \sum_k \boldsymbol{\sigma} : \mathbf{n}_{jk} \mathbf{n}_{jk} \right) \frac{N^{1/3}}{|\nabla\phi_i|} - \zeta \nabla^2 \phi_i \right] \dot{\phi}_i \\
& + \int_{\partial V} \left[\left(\frac{\partial\gamma}{\partial\Psi} + \kappa \mathbf{n} \cdot \nabla\Psi \right) \dot{\Psi} + \sum_i \zeta \mathbf{n} \cdot \nabla\phi_i \dot{\phi}_i \right] d\partial V.
\end{aligned}$$

The traction on the phase field level surface is $\boldsymbol{\sigma} \cdot \mathbf{n}_{ij}$. Only its tangential portion $\mathbf{t}_{ij}^t = \mathbf{P}_{ij} \cdot \boldsymbol{\sigma} \cdot \mathbf{n}_{ij}$ expands power on \mathbf{s}_{ij} . The normal traction on the phase field level surface is given as $t_{ij}^n = \mathbf{n}_{ij} \cdot \boldsymbol{\sigma} \cdot \mathbf{n}_{ij}$, and the overall normal traction field can be written as

$$t^n = \sum_j t_{jG}^n + \frac{1}{2} \sum_j \sum_k t_{jk}^n.$$

With those substitutions, we obtain

$$\begin{aligned}
\dot{\mathcal{F}} = & \int \left[-\frac{\partial(f+\mathcal{E})}{\partial\eta} \frac{1}{F^*} F^* \nabla \cdot \mathbf{q} + \left[\frac{1}{F^*} \frac{\partial(f+\mathcal{E})}{\partial\Psi} - \kappa \nabla^2 \Psi \right] \dot{\Psi} \right. \\
& + \left[\boldsymbol{\sigma} - \kappa(\nabla\Psi\nabla\Psi) - \sum_i \zeta(\nabla\phi_i\nabla\phi_i) \right] : (\mathbf{v}\nabla) - \frac{1}{2} \sum_i \sum_j \mathbf{t}_{ij}^t \cdot \mathbf{s}_{ij} \\
& + \sum_i \left[\frac{1}{F^*} \frac{\partial(f+\mathcal{E})}{\partial\phi_i} - \frac{1}{F^*} \frac{\partial(f+\mathcal{E})}{\partial\eta} \frac{\eta N^{1/3}}{|\nabla\phi_i|} - \frac{t^n N^{1/3}}{|\nabla\phi_i|} - \zeta \nabla^2 \phi_i \right] \dot{\phi}_i \\
& + \left. \int_{\partial V} \left[\left(\frac{\partial\gamma}{\partial\Psi} + \kappa \mathbf{n} \cdot \nabla\Psi \right) \dot{\Psi} + \sum_i \zeta \mathbf{n} \cdot \nabla\phi_i \dot{\phi}_i \right] d\partial v. \right]
\end{aligned}$$

Appendix C. Elimination of the Lagrange multiplier

$$\dot{\Psi} + \sum_i \dot{\phi}_i = 0 \quad \Rightarrow \quad -b_G \mathcal{M}^0 + (b_G + b_S n_g) \lambda - b_S \sum_i \mu_i^0 = 0$$

$$\Rightarrow \quad \lambda = \frac{b_G}{b_G + b_S n_g} \mathcal{M}^0 + \frac{b_S}{b_G + b_S n_g} \sum_j \mu_j^0,$$

$$\dot{\phi}_i = -b_S \mu_i^0 + \frac{b_S^2}{b_G + b_S n_g} \sum_j \mu_j^0 + \frac{b_S b_G}{b_G + b_S n_g} \mathcal{M}^0$$

$$\dot{\Psi} = \left(\frac{b_G^2}{b_G + b_S n_g} - 1 \right) \mathcal{M}^0 + \frac{b_G b_S}{b_G + b_S n_g} \sum_j \mu_j^0.$$

Appendix D. Equilibrium interface energy

Consider the equilibrium of two semi-infinite domains ($\Phi + \Psi = 1$) with the interface ($\Phi = \Psi = \frac{1}{2}$) located at $x = 0$. From (3.1) and (5.1), the interface energy is

$$(D.1) \quad \begin{aligned} \Gamma &= \int_{-\infty}^{\infty} \left[\Delta f w(\Phi) + \Delta f_G w(\Psi) + \frac{1}{2} \zeta \left(\frac{d\Phi}{dx} \right)^2 + \frac{1}{2} \kappa \left(\frac{d\Psi}{dx} \right)^2 \right] dx \\ &= \int_{-\infty}^{\infty} \left[(\Delta f + \Delta f_G) w(\Phi) + \frac{\zeta + \kappa}{2} \left(\frac{d\Phi}{dx} \right)^2 \right] dx. \end{aligned}$$

The equilibrium distribution $\Phi(x)$ that minimizes the interface energy, is obtained from the Euler equation:

$$(D.2) \quad (\Delta f + \Delta f_G) w(\Phi) = \frac{\zeta + \kappa}{2} \left(\frac{d\Phi}{dx} \right)^2,$$

which, upon the substitution in (D.1), gives

$$\begin{aligned} \Gamma &= \int_{-\infty}^{\infty} (\zeta + \kappa) \left(\frac{d\Phi}{dx} \right)^2 dx = \int_0^1 (\zeta + \kappa) \frac{d\Phi}{dx} d\Phi \\ &= \sqrt{2(\Delta f + \Delta f_G)(\zeta + \kappa)} \int_0^1 \sqrt{w(\Phi)} d\Phi = \frac{2}{3} \sqrt{2(\Delta f + \Delta f_G)(\zeta + \kappa)}. \end{aligned}$$

To obtain the nominal interface thickness, we solve differential equation (D.2) with $\Phi(0) = \frac{1}{2}$:

$$\begin{aligned} \frac{d\Phi}{dx} &= 4 \sqrt{\frac{2(\Delta f + \Delta f_G)}{\zeta + \kappa} \Phi(1 - \Phi)} \Rightarrow \ln \frac{\Phi}{1 - \Phi} = 4 \sqrt{\frac{2(\Delta f + \Delta f_G)}{\zeta + \kappa}} x \\ \frac{d\Phi}{dx} \Big|_{\Phi=1/2} &= \sqrt{\frac{2(\Delta f + \Delta f_G)}{\zeta + \kappa}} \Rightarrow h = \sqrt{\frac{\zeta + \kappa}{2(\Delta f + \Delta f_G)}}. \end{aligned}$$

References

1. R. J. Asaro, *Micromechanics of crystals and polycrystals*, Adv. Appl. Mech. **23** (1983), 1–115.
2. M. F. Ashby, *Materials Selection in Mechanical Design*, 4th ed., Elsevier, 2011.
3. J. L. Bassani, *Plastic flow of crystals*, Adv. Appl. Mech. **30** (1994), 191–257.
4. V. Berdichevsky, P. Hazzledine, B. Shoykhet, *Micromechanics of diffusional creep*, Int. J. Eng. Sci. **35** (1997), 1003–1032.
5. K. Chang, L.-Q. Chen, C.E. Krill III, N. Moelans, *Effect of strong nonuniformity in grain boundary energy on 3-D grain growth behavior: A phase-field simulation study*, Computational Materials Science **127** (2017), 67–77.
6. A. C. F. Cocks, M. F. Ashby, *On creep fracture by void growth*, Progress in Materials Science **27**(3–4) (1982), 189–244.
7. H. T. Davis, L. E. Scriven, *Stress and structure in fluid interfaces*, In: I. Prigogine, S. A. Rice (eds.), *Advances in Chemical Physics*, **49**, 357–454, Wiley, New York, 1982.
8. M. Dehsara, H. Fu, S. Dj. Mesarovic, D. P. Sekulic, M. Krivilyov, *(In)compressibility and parameter identification in phase field models for capillary flows*, Theor. Appl. Mech. **44**(2) (2017), 189–214.
9. P. Germain, *La méthode des puissances virtuelles en mécanique des milieux continus, 1ère partie: théorie du second gradient*, J. Méc., Paris **12** (1973), 235–274.

10. P. Germain, *The method of virtual power in continuum mechanics. Part 2: Microstructure*, SIAM J. Appl. Math. **25**(3) (1973), 556–575.
11. E. D. Guleryuz, S. Dj. Mesarovic, *Dislocation nucleation on grain boundaries: low angle twist and asymmetric tilt boundaries*, Crystals **6**(7) (2016), 77.
12. P. Haasen, *Physical Metallurgy*, 2nd ed., Cambridge University Press, Cambridge, UK, 1986.
13. R. Hill, K. S. Havner, *Perspectives in the mechanics of elastoplastic crystals*, J. Mech. Phys. Solids **30** (1982), 5–22.
14. M. Hillert, *On the theory of normal and abnormal grain growth*, Acta Metallurgica **13** (1965), 227–38.
15. J. P. Jaric, R. Vignjevic, S. Dj. Mesarovic, *Transport theorem for spaces and subspaces of arbitrary dimensions*, Mathematics **8**(6) (2020), 899.
16. S.-J. L. Kang, *Sintering*, 1st ed., Elsevier, Butterworth Heinemann, 2005.
17. S. Kovacevic, R. Pan, D. P. Sekulic, S. Dj. Mesarovic, *Interfacial energy as the driving force for diffusion bonding of ceramics*, Acta Materialia **186** (2020), 405–414.
18. S. Kovacevic, S. Dj. Mesarovic, *Diffusion-induced stress concentrations in diffusional creep*, Int. J. Solids Struct. **239–240** (2022), 111440.
19. L. E. Malvern, *Introduction to the Mechanics of a Continuous Medium*, Prentice-Hall, 1969.
20. J. Mandel, *Equations constitutives et directeurs dans les milieux plastiques et viscoplastiques*, Int. J. Solids Struct. **9**(6) (1973), 725–740.
21. S. Dj. Mesarovic, *Lattice continuum and diffusional creep*, Proc. R. Soc. Lond., A, Math. Phys. Eng. Sci. **472** (2016), 20160039.
22. S. Dj. Mesarovic, *Dislocation creep: Climb and glide in the lattice continuum*, Crystals **7**(8) (2017), 243.
23. S. Dj. Mesarovic, *Physical foundations of mesoscale continua*, In: S. Mesarovic, S. Forest, H. Zbib (eds), *Mesoscale Models: From Micro-Physics to Macro-Interpretation*, CISM International Centre for Mechanical Sciences **587**, 1–50, Springer, 2019.
24. S. Dj. Mesarovic, J. Padbidri, *Minimal kinematic boundary conditions for simulations of disordered microstructures*, Phil. Mag. **85**(1) (2005), 65–78.
25. E. Miyoshi, T. Takaki, *Multi-phase-field study of the effects of anisotropic grain-boundary properties on polycrystalline grain growth*, J. Crystal Growth **474** (2017), 160–165.
26. S. Ritchie, S. Kovacevic, P. Deshmukh, S. Dj. Mesarovic, R. Panat, *Shape distortion in sintering results from nonhomogeneous temperature activating a long-range mass transport*, Nature Communications **14** (2023), 2667.
27. H. Salama, J. Kundin, O. Shchyglo, V. Mohles, K. Marquardt, I. Steinbach, *Role of inclination dependence of grain boundary energy on the microstructure evolution during grain growth*, Acta Materialia **188** (2020), 641–651.

МЕХАНИКА ЧВРСТИХ ТЕЛА НА ПОВИШЕНИМ ТЕМПЕРАТУРАМА: РАЧУНСКА ФОРМУЛАЦИЈА НА МЕЋУНИВОУ

РЕИМЕ. Изведена је формулација фазног поља на међунивоу (између микро-нивоа (атоми) и макро-нивоа (велике запремине у инжењерским прорачунима)) за рачунски приступ механици чврстих тела на повишеним температурама. Математички опис укључује трансляцију и ротацију кристалних зрна, дифузију кроз кристале и међуповрши, раст кристалне решетке и клизање зрна на међуповршима, еластичне напоне и композиционе сопствене деформације. Формулација повезује хетерологне континууме; чврста тела су представљена континуумом решетке, док су празнине/гас представљени уобичајеним континуумом масе као вискозни (и запремински еластичан) флуид. Градијент деформације је стога променљива стања чија је еволуција дефинисана у Еулер-овском смислу. Посматрамо неинерцијалне процесе са контролисаном температуром, механизмом размене атома и празнина за дифузију и изотропним површинским енергијама. Упркос томе, као што је објашњено у Закљчцима, ова формулација даје основу за проширење теорије на процесе са значајним изворима и понорима топлоте, дифузију више врста атома и анизотропне површинске енергије.

School of Mechanical and Materials Engineering
Washington State University
Pullman
WA, USA
smesarovic@wsu.edu
<https://orcid.org/0000-0002-0117-426X>

(Received 05.06.2025)
(Revised 09.08.2025)
(Available online 16.09.2025)